

## Cronfa - Swansea University Open Access Repository

---

This is an author produced version of a paper published in :  
*Materials and Corrosion*

Cronfa URL for this paper:  
<http://cronfa.swan.ac.uk/Record/cronfa20511>

---

### Paper:

Yousef, H., Cobley, R., Davies, H., James, D., Mehmood, S., Sackett, E. & Sienz, J. Establishing a quantifiable tarnish timeline for comparison of anti-tarnish processes in metals. *Materials and Corrosion*, n/a-n/a.

<http://dx.doi.org/10.1002/maco.201407969>

---

This article is brought to you by Swansea University. Any person downloading material is agreeing to abide by the terms of the repository licence. Authors are personally responsible for adhering to publisher restrictions or conditions. When uploading content they are required to comply with their publisher agreement and the SHERPA RoMEO database to judge whether or not it is copyright safe to add this version of the paper to this repository.

<http://www.swansea.ac.uk/iss/researchsupport/cronfa-support/>

# **Establishing a quantifiable tarnish timeline for comparison of anti-tarnish processes in metals**

Haitham N. S. Yousef\*<sup>1</sup>, Richard J. Copley<sup>2</sup>, Helen M. Davies<sup>1</sup>, D. Matthew James<sup>3</sup>,  
Shahid Mehmood<sup>1</sup>, Elizabeth Sackett<sup>1</sup> and Johann Sienz<sup>1</sup>

<sup>1</sup> Advanced Sustainable Manufacturing Technologies (ASTUTE), College of Engineering, Swansea University, Singleton Park, Swansea SA2 8PP, UK

<sup>2</sup> Multidisciplinary Nanotechnology Centre, College of Engineering, Swansea University, Singleton Park, Swansea SA2 8PP, UK

<sup>3</sup> Royal Mint, Llantrisant, Pontyclun CF72 8YT, UK

\* [h.yousef@swansea.ac.uk](mailto:h.yousef@swansea.ac.uk) – Fax: +44-1792-513714

This is the accepted version of the following article:

Materials and Corrosion (2015) DOI: 10.1002/maco.201407969

which has been published in final form at

<http://onlinelibrary.wiley.com/doi/10.1002/maco.201407969/abstract;jsessionid=7E7F87FD0C104133B6C293386A2A0BEF.f01t03> .

## **Abstract**

Brass samples were controllably tarnished using the thioacetamide accelerated corrosion (ISO 4538:1995) and synthetic sweat (ISO 3160-2:2003) methods. Spectrophotometry, energy dispersive X-ray spectroscopy (EDX) and electrochemical impedance spectroscopy (EIS) were performed on samples tarnished for set exposure times over seven days. Synthetic sweat produced a loose surface corrosion layer, which limited the use of EIS and spectrophotometry, but for the thioacetamide method both measurements produced a continuous change over the time period. EDX was able to observe a continuous change in the surface layer chemistry for both methods over the whole timescale and represents the best characterisation method to establish an equivalent tarnish timeline against which anti-tarnish treated samples can be compared. The current study was conducted using brass, however the method can be used for quantifying tarnish on other metallic systems.

## **Keywords**

Tarnish quantification, spectrophotometry, ISO 3160-2:2003, ISO 4538:1995, EDX, EIS, artificial sweat, thioacetamide.

## **1 Introduction**

Tarnish affects many metals and alloys, and in order to compare anti-tarnish methods, a quantitative method is needed to describe the equivalent tarnish compared to baseline samples tarnished using ISO standard methods. We establish such a baseline in order that samples can be compared, using the example of brass.

Brass is an alloy of primarily copper and zinc, with zinc content varying from 5 to 45%. Small amounts of other elements can be added to improve the properties. For example, adding lead (up to 3%) improves machinability, whereas tin (0.4 to 1.5%) improves corrosion resistance, and iron (0.75 to 2.5%) improves yield strength [1].

Brass is a fundamental alloy for industry and has been utilised for many decades in the manufacture of electrical equipment, heat transfer equipment, domestic plumbing, seawater lines, gears, pinions and bearings due to its good thermal, corrosion and mechanical properties. It is also approved for use in hazardous environments because it does not spark when struck with other metals, and it has anti-bacterial properties where tests have shown its superiority in controlling harmful microorganisms. As well as industrial uses, brass has also been used for costume jewellery and decorative trim due to the attractive golden colour. [1-3].

Brass, like many other metals tarnishes in moist environments and its shiny golden colour progressively turns to darker brown and ultimately to green. The colour change is due to the formation of a layer of tarnish by-products when copper reacts with oxygen, chloride and sulphides. Tarnishing is undesirable in some applications such as jewellery because of loss of colour and shine, and in electrical equipment because it can cause failure of electrical connections [4,5]. To prevent this from happening, different types of coatings have been applied to improve tarnish resistance of brass [5-14]. However, no standard tests are available which can be used to predict the reliability of such tarnish resistance coatings or quantify the amount of tarnish produced.

To establish a quantifiable tarnish timeline for materials, brass was investigated. In the current work, three quantitative measures of tarnish resulting from two different ISO standard corrosion processes are established, which allow a quantifiable tarnish timeline to be established. This serves two purposes: firstly, anti-tarnish methods can be compared against each other quantitatively; secondly, products in circulation can be tested and compared to an equivalent exposure time in each ISO standard test. The current methodology is applicable to other tarnish testing techniques and other metals and alloys.

## **2 Experimental**

### **2.1 Materials & ISO Corrosion Methods**

The brass samples used in this study comprised of 73% copper and 27% zinc composition. They were tarnished in a controlled environment using two standard methods: the thioacetamide accelerated corrosion test (ISO 4538:1995) [15] and the synthetic perspiration (sweat) test (ISO 3160-2:2003) [16].

For the thioacetamide Accelerated Corrosion test (ACT), the brass samples were exposed to sulphide gases emitted by thioacetamide in a 75% relative humidity atmosphere maintained by a saturated sodium acetate solution at  $20\pm5^{\circ}\text{C}$ , in a sealed glass chamber. For the synthetic sweat test (SST), the brass samples were sprayed with a mist of synthetic sweat (Table 1) and placed in a sealed glass chamber at  $40\pm2^{\circ}\text{C}$ .

Samples were exposed to the ACT and SST tarnishing agents for 8 hours, 1 day, 3 days and 7 days. The maximum exposure time was selected after noticing the high discolouration of the samples after 7 days exposure.

Control samples, which had been stored in a protective environment, were also characterized to establish a baseline.

### **2.2 Analysis methods**

Colour measurements were performed using an X-Rite SP64 spectrophotometer and reported as CIE  $L^*C^*h^{\circ}$  triplets where  $L^*$  is the sample lightness,  $C^*$  is the sample chroma or colour saturation, and  $h^{\circ}$  is the sample hue or colour. The settings used were CIE D65/10° where D65 stands for daylight illuminant and 10° is the field of view or observer angle. Specular reflection was included [17].

EDX analysis was performed at a minimum of six locations using a Jeol 35C scanning electron microscope (SEM) and Oxford Instruments Aztec EDX analyser. SEM images were acquired using a Jeol 6100 SEM.

EIS measurements were performed using a CH Instruments' CHI 760E Electrochemical Workstation. A Platinum electrode was employed as the counter electrode, and a silver chloride (Ag/AgCl) electrode as the reference electrode. A frequency range of 1 Hz to 1 MHz, along with an AC Voltage of 5 mV was utilised for all experiments. Twelve measuring points were recorded in each frequency cycle between 1 Hz and 10 kHz, and fifty measuring points were logged in each frequency cycle between 10 kHz and 1 MHz. Impedance data was fitted for an equivalent  $1 \text{ cm}^2$  area to a simplified Randles cell (Fig. 1) where  $R_s$  is the solution resistance,  $R_{ct}$  is the charge transfer resistance and  $C_{dl}$  is the double layer capacitance [18].

### 3 Results and Discussion

#### 3.1 Colour measurements

Table 2 shows the colour timeline results for the two tarnishing methods. The same data is represented graphically in Fig. 2 and Fig. 3. Table 2 also shows the colour difference values in CIEDE2000 units ( $\Delta E_{00}^*$ ) [19]. The results for the tarnished samples represented the average of eight measurements. Fig. 4, Fig. 5 and Fig. 6 show SEM images at 20X magnification for control, ACT (7 days exposure) and SST (7 days exposure) samples; respectively.

For the ACT tarnishing method there was a clear trend in the results, which showed that as exposure time increased all colour components decreased over the full time scale. As a result, the tarnished samples' colour became darker, less saturated and moved towards red and away from yellow.

For the SST tarnishing method there was a trend observed in all colour components where values decreased over short exposure times up to one day. Beyond that, there was no significant change. The SST method was observed to form an uneven surface layer, which was not well adhered to the substrate and in some places peeled or cracked before

observation to reveal the less-tarnished substrate. This is partly responsible for the reduced colour change, but also the SST method appears to be self-limiting after 1 day.

SST is a liquid phase process where a fine mist is sprayed on to the sample. Coalescence of the droplets in the mist and the resulting non-uniform coating could explain the uneven surface layer as can be seen clearly in Fig. 6. In comparison the vapour phase ACT method produced a much more uniform, compact and mechanically stable surface layer as can be demonstrated in Fig. 5 and is similar to the control sample surface, Fig. 4.

### 3.2 EDX measurements

Results for the EDX timeline are shown in Fig. 7 and Fig. 8.

It can be observed from the plots that as exposure time increases for both methods, tarnish by-products (oxygen, sulphur and chlorine) increase. However copper and zinc were seen to decrease as a weight fraction due to the increase in other species. An evaluation between the two methods of tarnishing demonstrated that the SST tarnishing method illustrated larger changes in copper and oxygen weight fractions compared to the ACT tarnishing method. These rapid weight fractions changes in the SST results are attributed to the higher temperature of the SST tarnishing method ( $40\pm 2^\circ\text{C}$ ) as compared to ACT tarnishing method ( $20\pm 5^\circ\text{C}$ ) [20].

### 3.3 EIS measurements

Fig. 9 and Fig. 10 show  $R_{ct}$  timelines for ACT and SST experiments; respectively. Fig. 11 and Fig. 12 show  $C_{dl}$  timelines for ACT and SST experiments; respectively.

For ACT there is a general trend of increasing parallel resistance  $R_{ct}$  and decreasing capacitance  $C_{dl}$  over the whole timeline. This is attributed to the increased surface coverage by tarnish by-products, which did not saturate over a period of seven days.

The SST method showed no trend over the whole time period. For SST, surface changes went beyond tarnishing towards corrosion. This however had no impact on the primary  $R_{ct}$  and  $C_{dl}$

curves fitted here, probably because the surface change caused by the SST method is either not large enough to significantly alter surface electrical measurements, or is indicative of a porous or loose coating [5,8] which was observed in some samples with the corresponding additional time-constant in the EIS response. The formation of a porous or loose coating is suggestive of corrosion instead of tarnish [21].

## **4 Conclusions**

Brass samples were controllably tarnished using two ISO standard accelerated corrosion methods: accelerated corrosion (ACT) and synthetic sweat (SST). Surface analysis methods were applied as a function of time to establish an equivalent tarnish timeline.

The ACT method produced a uniform, compact and mechanically stable surface layer while the SST method produced a non-uniform, porous or loose and less mechanically stable surface layer. The nature of the surface layer formed by the SST method is indicative of corrosion, rather than tarnish, resulting from exposure to synthetic sweat.

Spectrophotometry measured colour changes over the first day of exposure for both ACT and SST, but colour changes saturated after 1 day for SST. For ACT colour changes continued over the full 7 day duration.

EIS measurements showed an increase in charge transfer resistance and a corresponding reduction in double layer capacitance over the full timeline for the ACT method, however no trend was observed for SST.

EDX surface chemical composition measurements changed over the full 7-day duration for both ACT and SST.

For the ACT method, results from all three analyses methods can be used to construct tarnish time lines however for the SST method, only EDX results can be used to construct a tarnish time line. EDX is clearly the preferred method to show a trend over a period of at least seven days equivalent exposure for both the ACT and SST methods. Samples with anti-tarnish



treatments can then be compared back to this timeline, to give an equivalent exposure time for an untreated sample.

### **Acknowledgements**

The authors acknowledge the financial support from the EU's Convergence European Regional Development Fund through the Welsh Government for ASTUTE to facilitate this work.

The authors wish to thank the Royal Mint for providing the samples used in this study.

## References

- [1] K. Kempson, *Eng. Des.* **2004**, *May/June*, 1.
- [2] Copper Development Association, "The Brasses: Properties and Applications," [Online]. Available: [http://admin.copperalliance.eu/docs/librariesprovider3/pub-117---the-brasses\\_whole\\_web-pdf.pdf?sfvrsn=0&sfvrsn=0](http://admin.copperalliance.eu/docs/librariesprovider3/pub-117---the-brasses_whole_web-pdf.pdf?sfvrsn=0&sfvrsn=0). [Accessed 8 8 2014].
- [3] A. J. Varkey, *Sci. Res. Essays* **2010**, *5*, 3834.
- [4] D.-Q. Zhang, H. G. Joo, K. Y. Lee, *Surf. Interface Anal.* **2008**, *41*, 164.
- [5] P. Wang , C. H. Liang, J. Zhang, *Mater. Corros.* **2007**, *58*, 604.
- [6] S. Chaudhari, A. B. Gaikwad, P. P. Patil, *Curr. Appl. Phys.* **2009**, *9*, 206.
- [7] M. Es-saheb, E.-S. M. Sherif, A. El-Zatahry, M. M. El Rayes, K. A. Khalil, *Int. J. Electrochem. Sci.* **2012**, *7*, 10442.
- [8] H. Q. Fan, S. Y. Li, Z. C. Zhao, H. Wang, Z. C. Shi, *Mater. Corros.* **2011**, *62*, 1133.
- [9] H. Fan, S. Li, Z. Shi, X. Lv, Z. Zhao, *Anti-Corros. Methods Mater.* **2012**, *59*, 32.
- [10] T. Harada, H. Nakanishi, T. Ogata, Y. Kadotani, A. Izumi, *Thin Solid Films* **2011**, *519*, 4487.
- [11] C. Liang, P. Wang, B. Wu, N. Huang, *Mater. Corros.* **2011**, *62*, 53.
- [12] S. Zor, H. I. Ünal, H. M. Gökergil, *Prot. Met. Phys. Chem. Surf.* **2011**, *47*, 813.
- [13] D. Patil, P. P. Patil, *J. Appl. Polym. Sci.* **2010**, *118*, 2084.
- [14] T.-L. Wang, W.-S. Hwang, M.-H. Yeh, *J. Appl. Polym. Sci.* **2007**, *104*, 4135.
- [15] *ISO 4538:1995: Metallic Coatings - Thioacetamide Corrosion Test (TAA Test)*, **1995**.
- [16] *ISO 3160-2:2003: Watch-Cases and Accessories - Gold Alloy Coverings - Part 2: Determination of Fineness, Thickness, Corrosion Resistance and Adhesion*, **2003**.
- [17] X-Rite, Inc., "A Guide to Understanding Color Communication," [Online]. Available: [http://www.xrite.com/documents/literature/en/L10-001\\_Understand\\_Color\\_en.pdf](http://www.xrite.com/documents/literature/en/L10-001_Understand_Color_en.pdf). [Accessed 8 8 2014].

- [18] Gamry Instruments, “Basics of Electrochemical Impedance Spectroscopy,” [Online]. Available: <http://www.gamry.com/application-notes/basics-of-electrochemical-impedance-spectroscopy/>. [Accessed 8 8 2014].
- [19] *ISO 11664-6:2014: Colorimetry – Part 6: CIEDE2000 Colour-Difference Formula*, **2014**.
- [20] G. Kılınççeker, *Colloids Surf., A* **2008**, 329, 112.
- [21] J. R. Davis, *Corrosion: Understanding the Basics*, ASM International, Novelty OH USA, **2000**.

## List of Figures

Fig. 1 – Simplified Randles Circuit.

Fig. 2 – CIE  $L^* C^* h^\circ$  tarnish timeline for the ACT method with standard error bars

Fig. 3 – CIE  $L^* C^* h^\circ$  tarnish timeline for the SST method with standard error bars.

Fig. 4 – SEM image of control sample.

Fig. 5 – SEM image of ACT 7 days exposure sample.

Fig. 6 – SEM image of SST 7 days exposure sample.

Fig. 7 – EDX tarnish timeline for ACT method with standard error bars.

Fig. 8 – EDX tarnish timeline for SST method with standard error bars.

Fig. 9 – ***Rct*** tarnish timeline for ACT method with standard error bars.

Fig. 10 – ***Rct*** tarnish timeline for SST method with standard error bars.

Fig. 11 – ***Cdl*** tarnish timeline for ACT method with standard error bars.

Fig. 12 – ***Cdl*** tarnish timeline for SST method with standard error bars.

## List of Tables

Table 1 – Synthetic sweat composition [16].

Table 2 – CIE  $L^* C^* h^\circ$  ( $\pm$  standard error) and  $\Delta E_{00}^*$  tarnish timelines for ACT and SST methods.

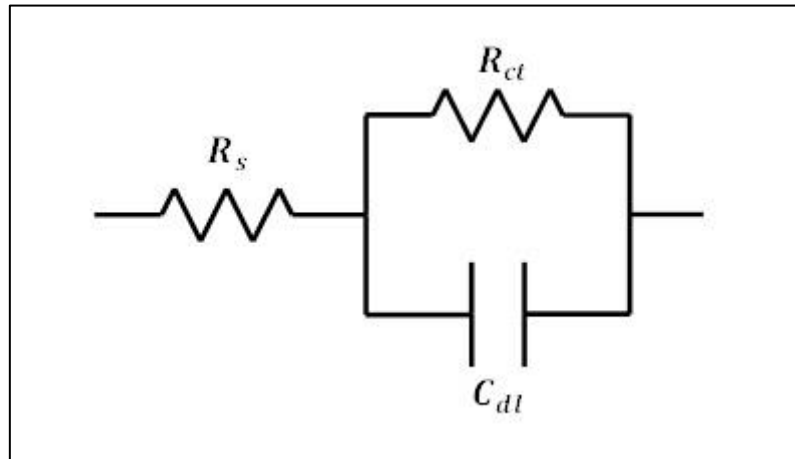


Fig. 1 – Simplified Randles Circuit.

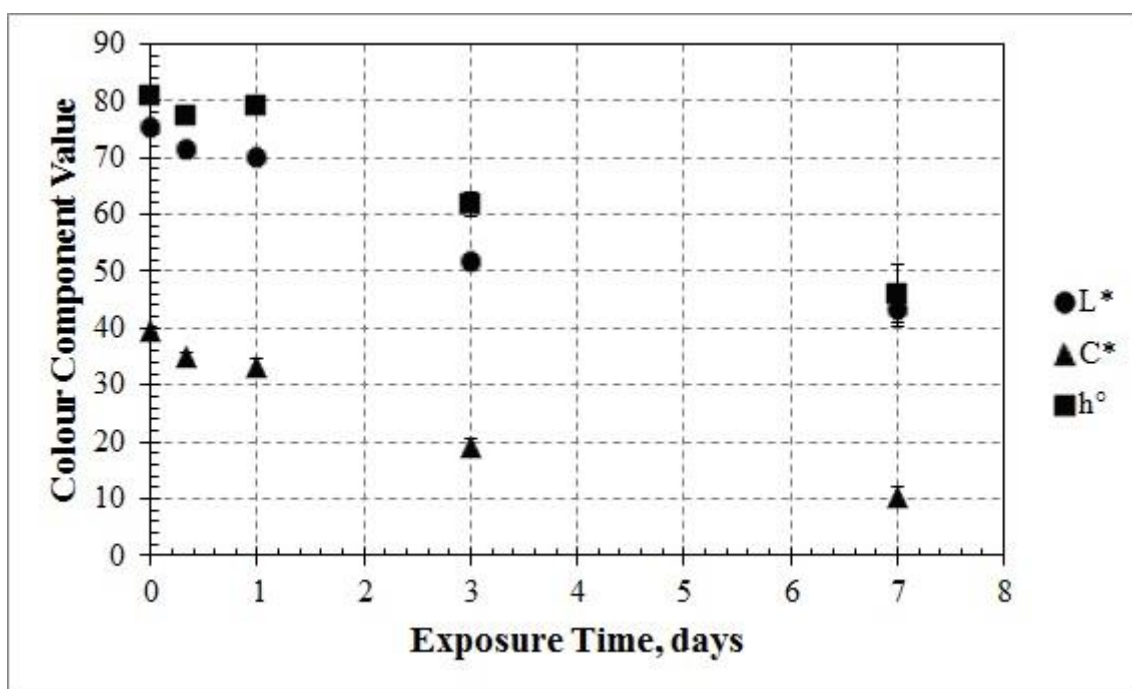


Fig. 2 – CIE  $L^*C^*h^\circ$  tarnish timeline for the ACT method with standard error bars

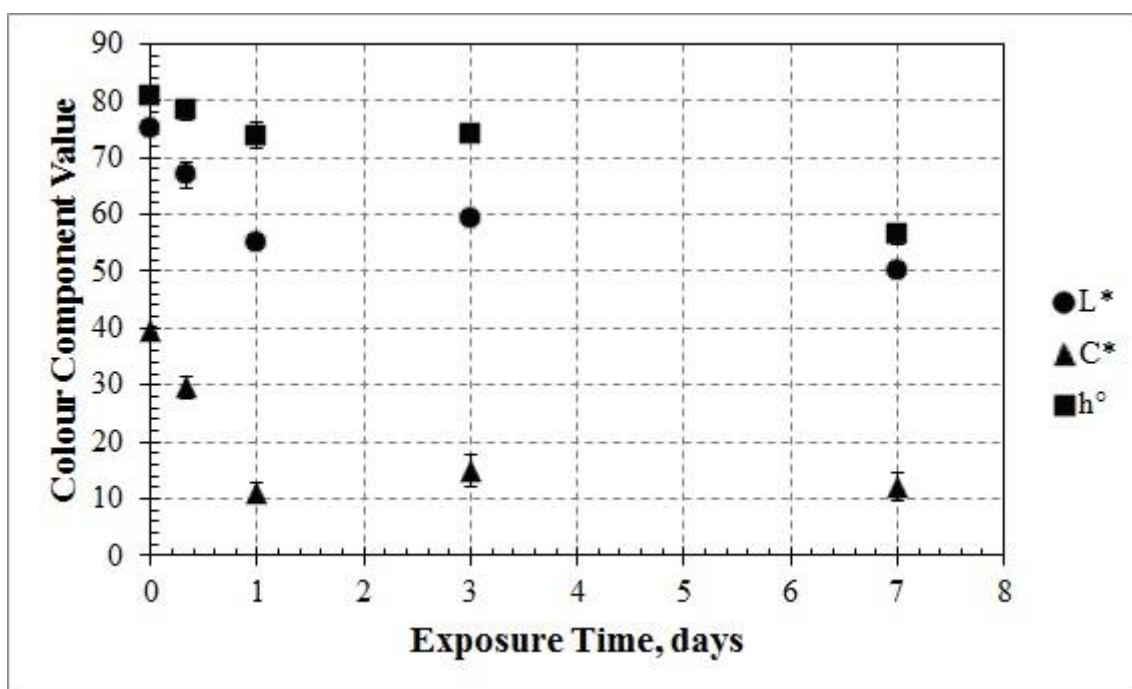


Fig. 3 – CIE  $L^*C^*h^\circ$  tarnish timeline for the SST method with standard error bars.



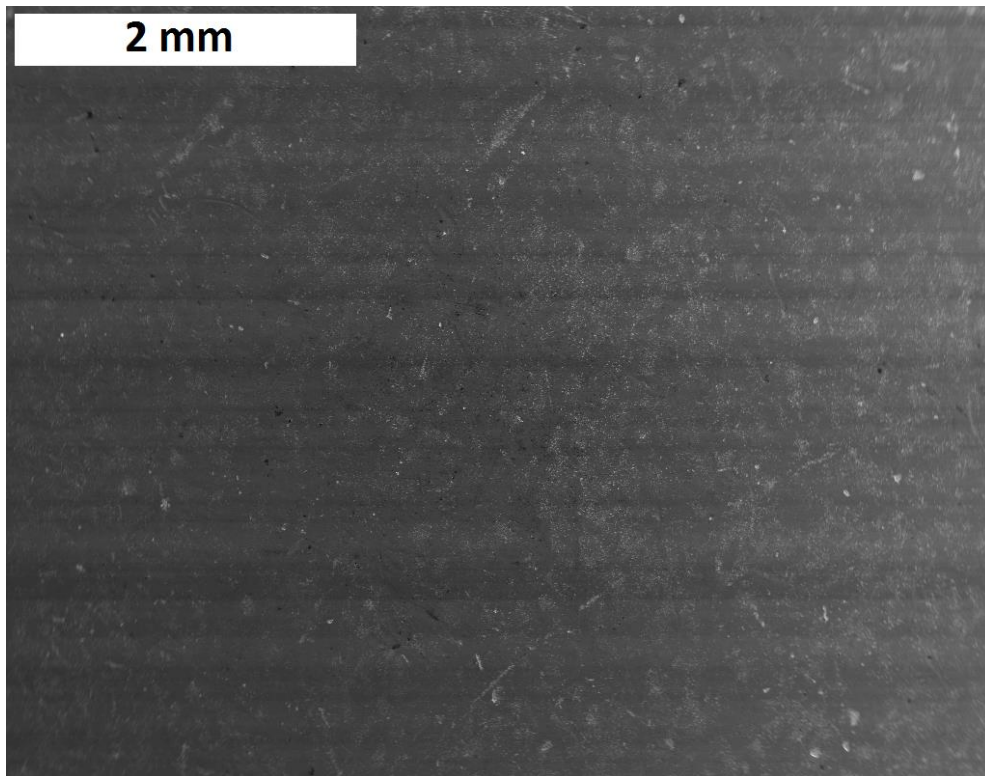


Fig. 4 – SEM image of control sample.

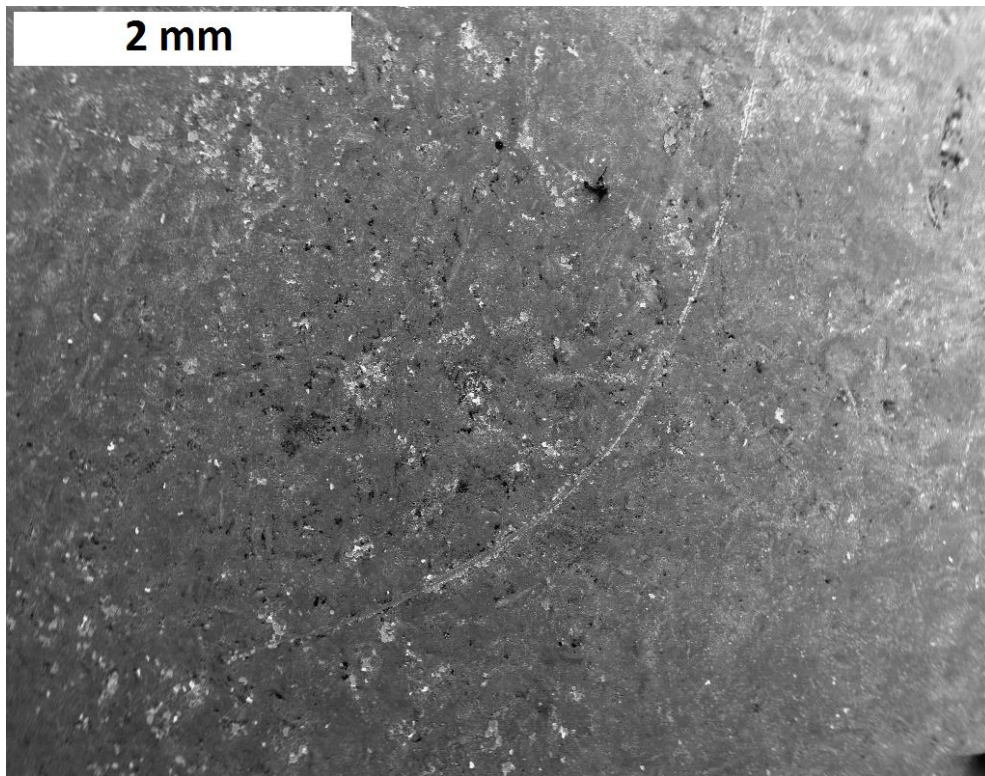


Fig. 5 – SEM image of ACT 7 days exposure sample.

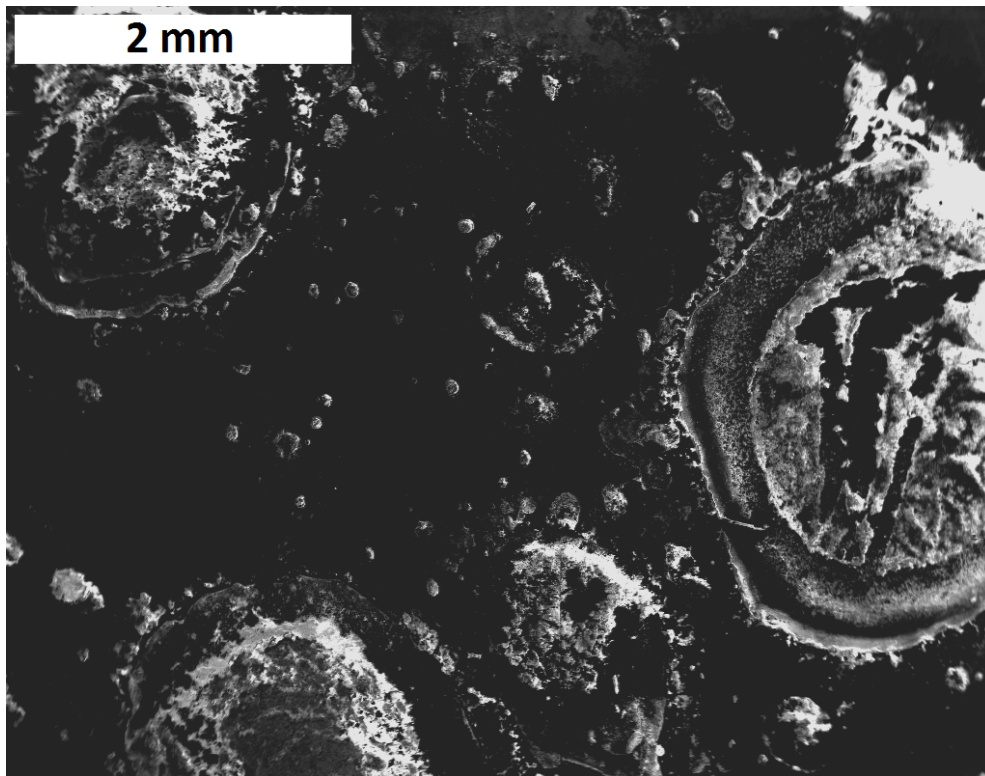


Fig. 6 – SEM image of SST 7 days exposure sample.

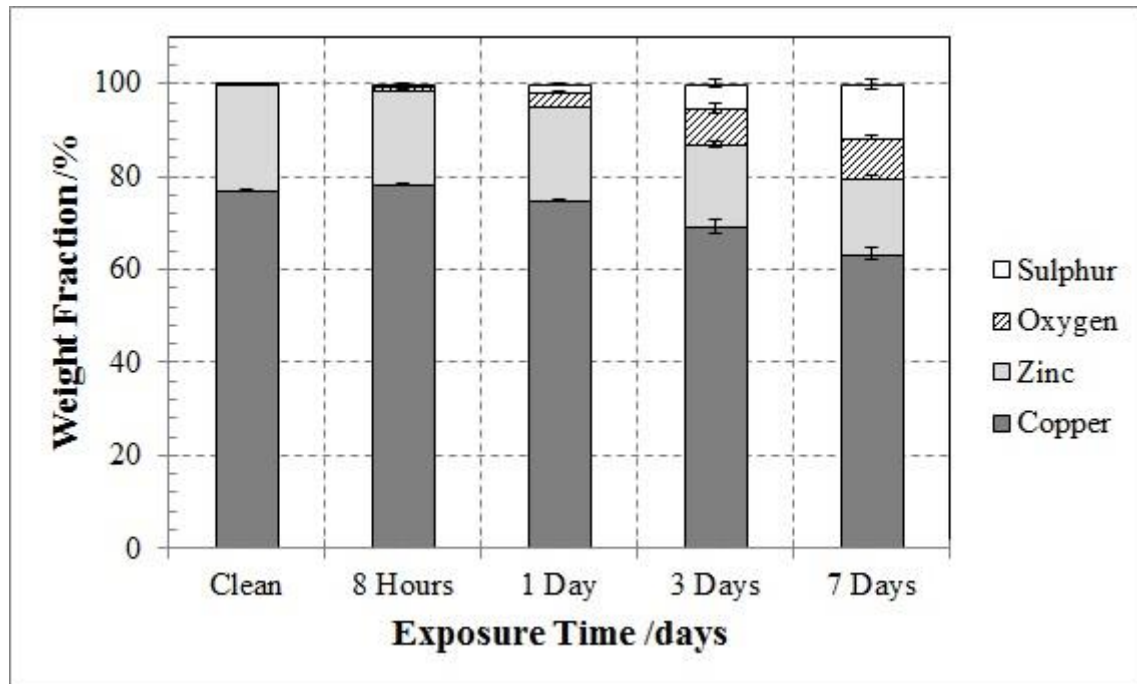


Fig. 7 – EDX tarnish timeline for ACT method with standard error bars.

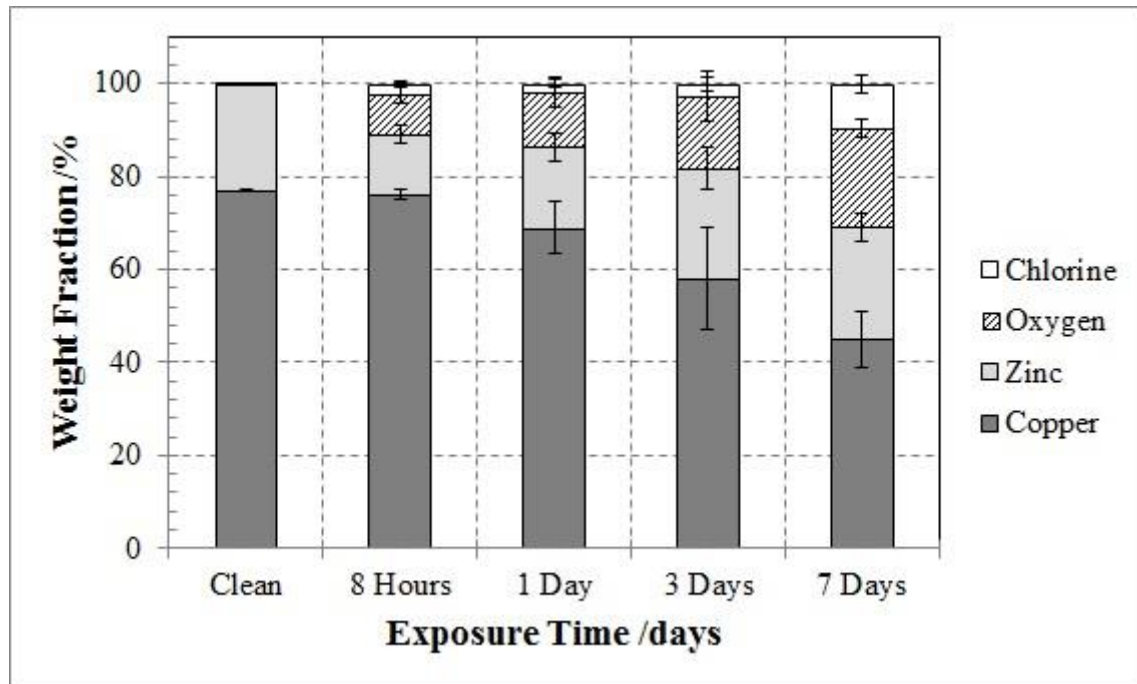


Fig. 8 – EDX tarnish timeline for SST method with standard error bars.

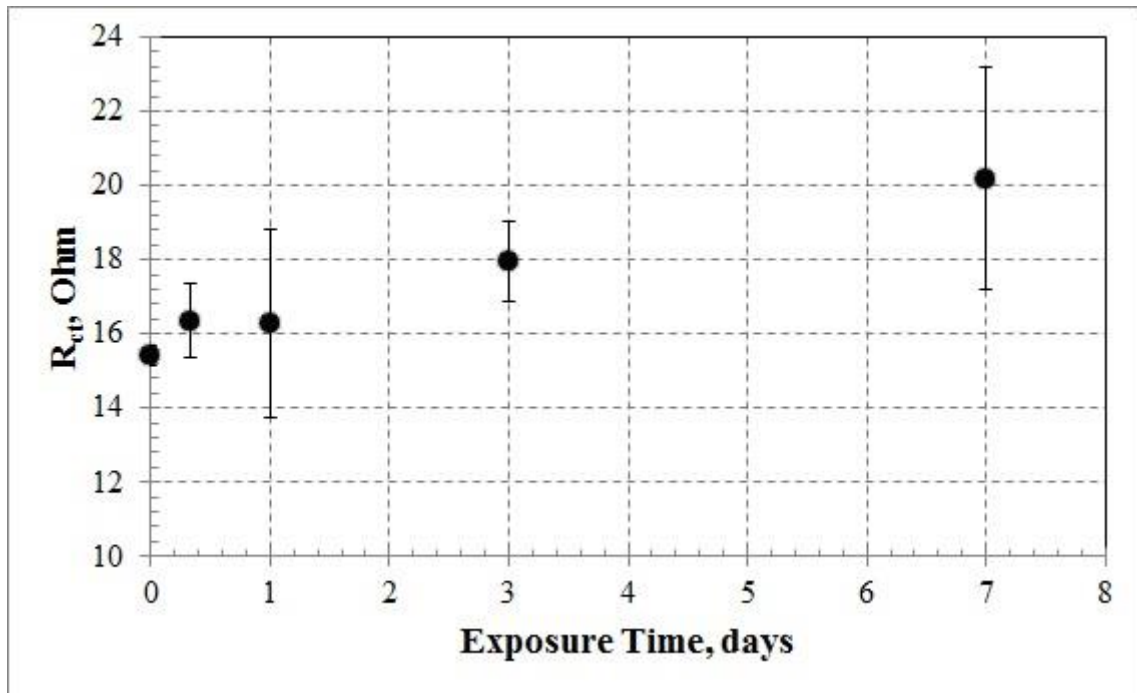


Fig. 9 –  $R_{ct}$  tarnish timeline for ACT method with standard error bars.

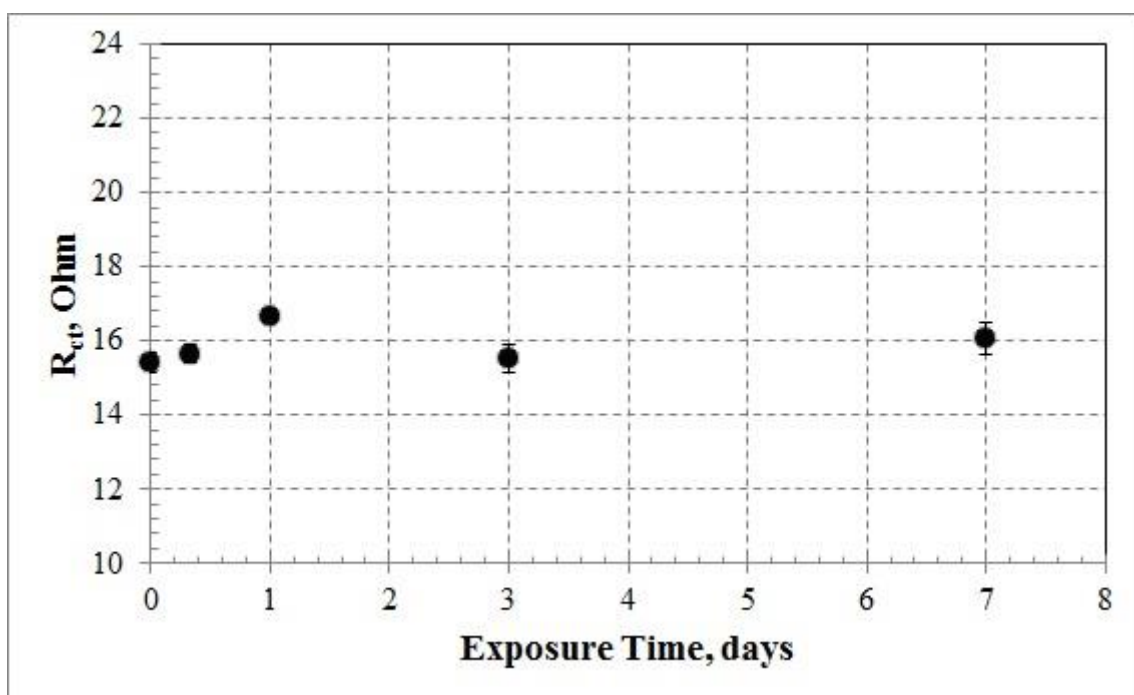


Fig. 10 –  $R_{ct}$  tarnish timeline for SST method with standard error bars.

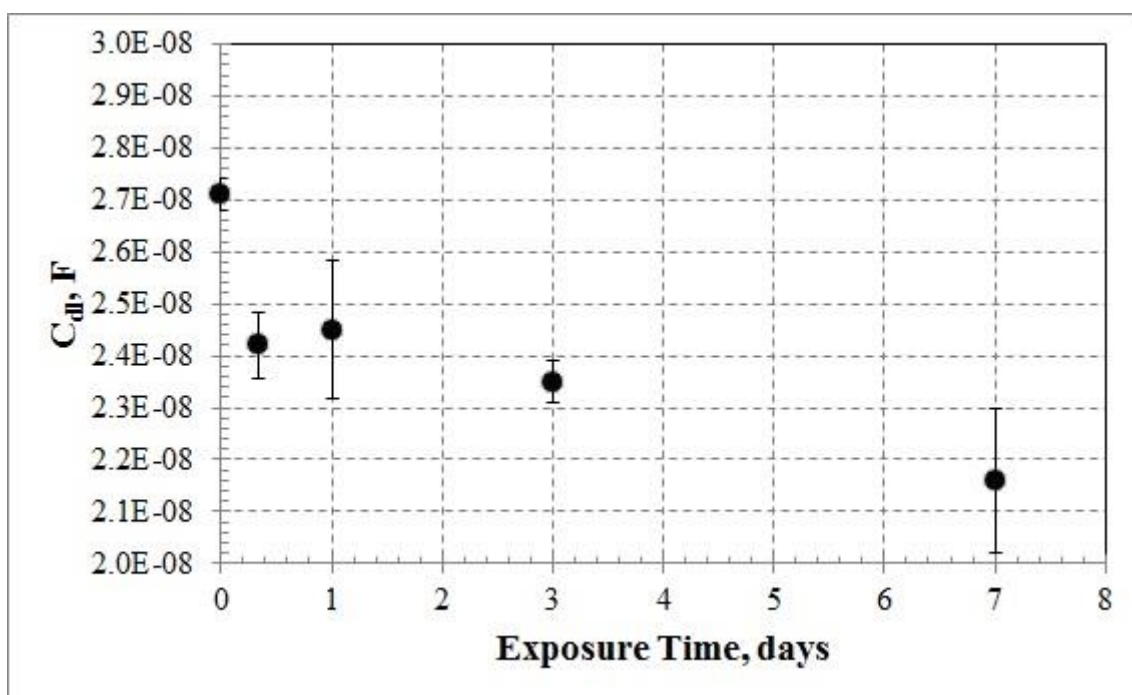


Fig. 11 –  $C_{dl}$  tarnish timeline for ACT method with standard error bars.



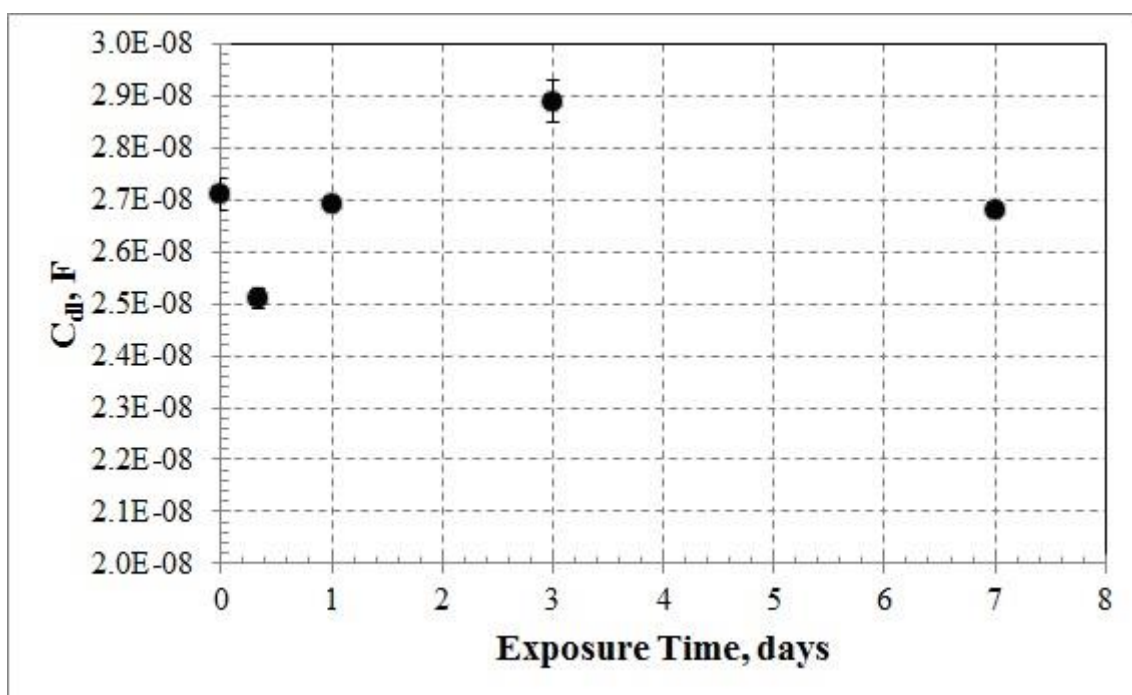


Fig. 12 –  $C_{dl}$  tarnish timeline for SST method with standard error bars.

Table 1 – Synthetic sweat composition [16].

<b>Chemical compound</b>	<b>Concentration, g/L</b>
Sodium chloride	20
Ammonium chloride	17.5
Urea	5
Acetic acid	2.5
Racemic lactic acid	15
Sodium hydroxide	Added to bring pH to 4.7

Table 2 – CIE  $L^*C^*h^\circ$  ( $\pm$  standard error) and  $\Delta\bar{E}_{00}^*$  tarnish timelines for ACT and SST methods.

Tarnishing Method	Exposure Time Days	$L^*$	$C^*$	$h^\circ$	$\Delta\bar{E}_{00}^*$
	0.00	$75.18 \pm 0.51$	$39.73 \pm 0.66$	$80.97 \pm 0.41$	0.00
ACT	0.33	$71.31 \pm 1.11$	$34.95 \pm 0.82$	$77.24 \pm 1.03$	16.99
ACT	1.00	$69.99 \pm 0.82$	$33.07 \pm 1.47$	$79.19 \pm 1.02$	18.27
ACT	3.00	$51.54 \pm 1.17$	$19.31 \pm 1.33$	$61.73 \pm 2.11$	28.57
ACT	7.00	$42.94 \pm 2.09$	$10.45 \pm 1.54$	$45.88 \pm 5.50$	38.11
SST	0.33	$66.92 \pm 2.28$	$29.57 \pm 2.01$	$78.35 \pm 1.88$	19.78
SST	1.00	$55.17 \pm 0.96$	$11.00 \pm 1.85$	$73.93 \pm 2.35$	29.43
SST	3.00	$59.45 \pm 0.85$	$14.86 \pm 2.90$	$74.20 \pm 1.06$	26.14
SST	7.00	$50.07 \pm 1.02$	$12.05 \pm 2.51$	$56.38 \pm 1.58$	32.05